DEPARTAMENTO DE CIÊNCIAS DA VIDA

FACULDADE DE CIÊNCIAS E TECNOLOGIA
UNIVERSIDADE DE COIMBRA

High-Resolution Respirometry for Metabolic Profiling of Acute Rat Hippocampal Slices

Tiago André Ferreira Henriques

2013

Tiago André Ferreira Henriques High-Resolution Respirometry for Metabolic Profiling of Acute Rat Hippocampal Slices 2013

DEPARTAMENTO DE CIÊNCIAS DA VIDA

FACULDADE DE CIÊNCIAS E TECNOLOGIA
UNIVERSIDADE DE COIMBRA

High-Resolution Respirometry for Metabolic Profiling of Acute Rat Hippocampal Slices

Dissertação apresentada à Universidade de Coimbra para cumprimento dos requisitos necessários à obtenção do grau de Mestre em Bioquímica, realizada sob a orientação científica do Professor Doutor João Laranjinha (Universidade de Coimbra, Faculdade de Farmácia) e da Doutora Ana Ledo (Centro de Neurociências e Biologia Celular), com supervisão institucional do Professor Doutor Carlos Palmeira (Universidade de Coimbra, Faculdade de Ciências e Tecnologia).

Tiago André Ferreira Henriques

2013

ACKNOWLEDGMENTS

Em primeiro lugar gostava de agradecer aos meus orientadores, o Professor Doutor João Laranjinha e à Doutora Ana Ledo, pela sua orientação, esforço e disponibilidade, e por me terem ajudado a crescer como pessoa e investigador durante este ano. Tenho de agradecer, especialmente, à Doutora Ana Ledo por me ter acompanhado durante este ano e me ter ajudado a resolver os problemas e entraves que foram aparecendo ao longo do percurso. Gostava de agradecer ao Professor Doutor João Laranjinha pela oportunidade de trabalhar no grupo de investigação "Redox Biology in Health and Disease" e por me ter ajudado no desenvolvimento da hipótese e desenho estratégico do trabalho feito ao longo do último ano.

Quero agradecer aos restantes membros do grupo de investigação "Redox Biology and Health and Disease" por terem contribuido para este tese através das trocas de ideias e discussões científicas, e através da partilha de conhecimentos e experiências.

Obrigado à minha família, não só por, a grande custo, me ter financiado o percurso académico, mas também e, principalmente, por terem estado lá nos momentos mais dificeis e sempre me terem apoiado incondicionalmente. Quero agradecer particularmente ao meu Tio Manuel por ter feito tudo ao seu alcance para que eu pudesse ter uma educação, apesar de eu muitas vezes não ter sabido retribuir.

Muito obrigado ao Caramelo, à Daniela, à Paula, ao Paulo, ao Ricardo Silva, ao Ricardo Oliveira e ao Tiago por nos últimos 5 anos terem ouvido as minhas ideias descabidas, e por partilharem as suas ideias descabidas. O pensamento crítico que desenvolvi durante as nossos argumentos foi-me muito útil ao longo desta trabalho. Obrigado também pelo vosso apoio, gargalhadas e camaradagem.

Obrigado aos 20 ratos que se sacrificaram por esta nobre causa, apesar de eles possivelmente desconhecerem este sentimento.

Esta tese não foi apenas um trabalho individual, mas sim fruto da ajuda e contribuição de todas as pessoas mencionadas e, por isso, estarei eternamente grato.

INDEX

ABBREVIATION INDEX

aCSF – Artificial cerebrospinal fluid

ADP – Adenosine diphosphate

ANLSH – Astrocyte neuron lactate shuttle hypothesis

ATP – Adenosine triphosphate

BBB – Blood brain barrier

BSA – Bovine serum albumin

CA – Cornu ammonis

CCCP – Carbonyl cyanide m-chloro phenyl hydrazone

cNOS – Constitutive nitric oxide synthase

DNP – 2,4-dinitrophenol

eNOS – Endothelial nitric oxide synthase

ETS – Electron transfer system

FADH2/FAD – Flavin adenine dinucleotide

FCCP – Carbonyl cyanide 4-(trifluoromethoxy)phenylhydrazone

FCR – Flux control ratio

FEP – Flurinated ethylene propylene

GLUT – Glucose transporter

HEPES – 4-(2-hydroxyethyl)-1-piperazineethanesulfonic acid

iNOS – Inducible nitric oxide synthase

IRF-1 – Interferon regulatory factor-1

Km – Michaelis constant

MCT – Monocarboxylate transporters

NADH/NAD+ – Nicotinamide adenine dinucleotide

NADPH/NADP+ - Nicotinamide adenine dinucleotide phosphate

NALSH – Neuron-to-astrocyte lactate shuttle hypothesis

NF-κB - Nuclear factor kappa-light-chain-enhancer of activated B cells

NMDA – N-Methyl-D-aspartate

nNOS – Neuronal nitric oxide synthase

NOS – Nitric oxide synthases

PSD-95 – Postsynaptic density protein-95

ROX – Residual oxygen consumption

RVI – Respiratory viability index

TCA – Tricarboxylic acid

TTFA – Thenoyltrifluoroacetone

TTFB – 4,5,6,7-tetrachloro-2-trifluoromethylbenzimidazole

FIGURE INDEX

ABSTRACT

There are still many unanswered questions in the field of brain bioenergetics and the question of which substrates normally fuel brain metabolism remains unresolved. In particular, it is not clear whether substrate preference is different between neurons and astrocytes, if this preference changes during increased neuronal activity or if the primary pathway to metabolize said substrate is aerobic glycolysis or the tricarbocylic acid (TCA) cycle.

Here we attempt to offer some insight on this problematic by performing high-resolution respirometry on acute hippocampal slices to evaluate tissue bioenergetics under different metabolic states. By using intact hippocampal slices, the intricate cellular interactions between neurons and astrocytes are maintained, as well as the neuronal circuitry, aspects that certainly have a critical role in the regulation of such metabolic pathways and crosstalks.

We show that activation of hippocampal slices by exogenous glutamate leads to an increase in oxidative metabolism, suggesting higher TCA cycle activity and little to no contribution of aerobic glycolysis. We also show that both basal and activity-induced increase of respiration in hippocampal slices can be fuelled by lactate. These results suggest that hippocampal cells readily use lactate as a substrate of oxidative metabolism and that even in the situation of increased neuronal activity, lactate is a good alternative to glucose.

As predicted, $^{\bullet}$NO titration decreased oxygen consumption rate (OCR) in acute rat hippocampal slices. This effect of nitric oxide on mitochondrial respiration has been showed in isolated mitochondria, synaptosomes and intact cells, but not in rat hippocampal slices, a model that maintains the neural cytoarchitecture and the functional cellular relationship between neurons and astrocytes.

Keywords: high resolution respirometry; slices; hippocampus; nitric oxide; neurometabolism.

SUMÁRIO

Ainda existem muitas questões por responder no campo da bioenergética cerebral e a questão de quais são os substratos que normalmente abastecem o metabolismo cerebral ainda não foi resolvida. Em particular, não é claro se a preferência por substratos é diferente entre neurónios e astrócitos, se essa preferência muda durante períodos de aumento da atividade neuronal ou se a via metabólica primária para metabolizar esse substrato é a glicólise aeróbia ou o ciclo dos ácidos tricarboxílicos (TCA).

Tentamos aqui contribuir para a compreensão desta problemática realizando respirometria de alta definição em fatias de hipocampo para avaliar a bioenergética do tecido em vários estados metabólicos. Usando fatias de hipocampo intactas, as intrincadas interações celulares entre neurónios e astrócitos são mantidas, assim como os circuitos neuronais, aspetos que certamente têm um papel crítico na regulação de vias metabólicas e interações.

Nós demonstramos que a ativação de fatias de hipocampo por glutamato exógeno leva ao aumento do metabolismo oxidativo, sugerindo maior atividade do ciclo TCA e pouca ou nenhuma contribuição da glicólise aeróbia. Demonstramos, também, que tanto a respiração basal como o aumento da respiração induzida pelo glutamato podem ser abastecidas pelo lactato. Estes resultados sugerem que as células do hipocampo possuem a podem usar lactato como substrato do metabolismo oxidativo e que mesmo numa situação de atividade neuronal aumentada, o lactato é uma alternativa à glucose.

Tal como previsto, a titulação de óxido nítrico ($^{\bullet}NO$) diminuiu a taxa de consumo de oxigénio (OCR) em fatias de hipocampo. Este efeito do $^{\bullet}NO$ já tinha sido descrito em mitocôndrias isoladas, sinaptossomas e células intactas, mas nunca em fatias de hipocampo de rato, um modelo que mantêm a citoarquitectura neuronal e a relação celular funcional entre neurónios e astrócitos.

Palavras-chave: respirometria de alta defenição; fatias; hipocampo; óxido nítrico; neurometabolismo.

1 INTRODUCTION

1.1 BIOENERGETICS OF THE BRAIN

Albeit comprising about 2% of the whole body mass, the human brain consumes around 20% of O_2 and 25% of the glucose[1] consumed in the body. Most of these resources are used for the phosphorylation of adenosine diphosphate (ADP) to adenosine triphosphate (ATP). A major contributor to this high energetic demand is the regulation of the membrane potential after neural depolarization, a process mediated by the Na^+/K^+-ATPase. Besides maintenance of regular cell function, neurotransmitter recycling and dendritic transport[2] are also major contributors to energy expenditure in the neuronal tissue.

The blood brain barrier (BBB) limits the access of many molecules, including metabolic substrates, to the brain tissue on the basis of polarity and size. The BBB is composed of endothelial cells connected by tight-junctions. This structure limits the diffusible molecules through the BBB to hydrophobic molecules like O_2, CO_2 and corticosteroids[3]. Non-hydrophobic molecules, cross the BBB through specific channels and transporters expressed by the endothelial cells. Regarding metabolic substrates, endothelial cells have transporters for glucose, amino acids, lactate, pyruvate and ketone bodies[4].

Astrocytes can store a limited amount of glycogen, however, this reserve can only sustain the brain metabolic requirements for a few minutes[5]. This means that the brain tissue has to rely on the bloodstream to supply metabolic substrates to fuel its metabolic activity.

1.1.1 Metabolic Substrates of the Brain

Since the inception of the field of brain energetics, glucose has been considered the primary substrate for both neurons and glia[6]. The conventional theory of brain metabolism (figure 1) states that upon increased metabolic demand in the brain tissue both astrocytes and neurons oxidize glucose to meet their energetic demands.

Production of lactate in this situation is atributed to the production of glycolitic products that exceeds the capacity of oxidative phosphorilation, and both astrocytes and neurons secrete such products to the bloodstream in the form of lactate[7]. Under this scope, lactate is considered a metabolic dead point.

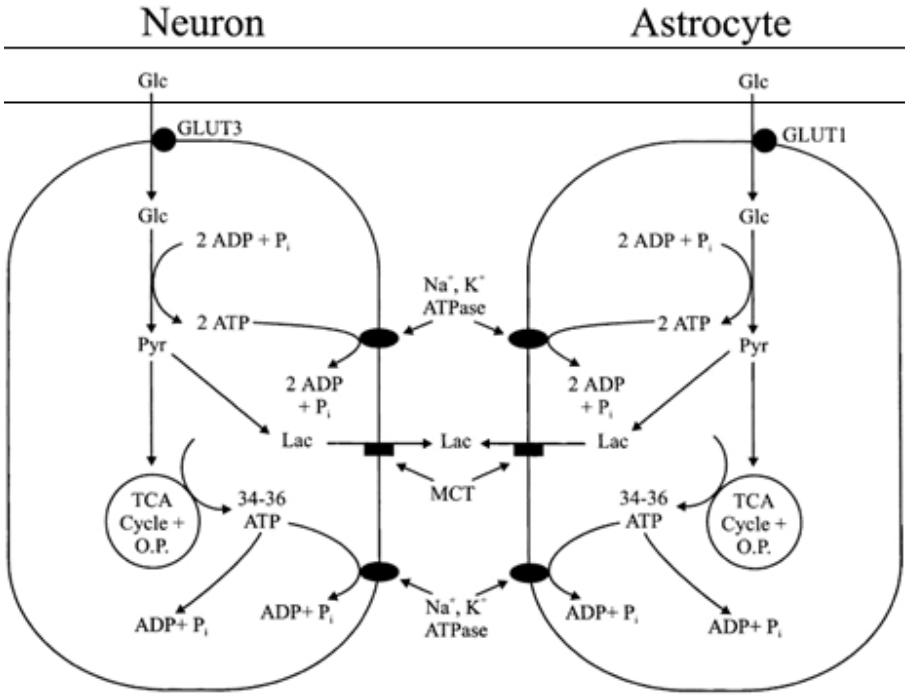

Figure 1. Schematic representation of glucose metabolism in neurons and astrocytes during increased neural activity, according to the conventional hypothesis. Adapted from Chih and Roberts Jr, 2003.

A few years ago a new theory that contradicts this early assumption was proposed by Pellerin and Magistretti: the astrocyte-neuron lactate shuttle hypothesis (ANLSH). The ANLSH proposed that, at least under certain circumstances, the astrocytes metabolize glucose to lactate, in a process called aerobic glycolysis. This lactate is then shuttled to neurons to fuel oxidative phosphorylation[8].

In accordance with the ANLSH, following glutamatergic activity, glutamate uptake by astrocytes activates glycolytic enzymes. The astrocytes increase their glucose uptake and metabolize it to lactate through aerobic glycolysis. In the light of this theory, neurons are incapable of increasing glycolytic activity to support increased energy demand. They use the lactate released by the astrocytes and oxidize it in the mithochondria[9,10] (figure 2).

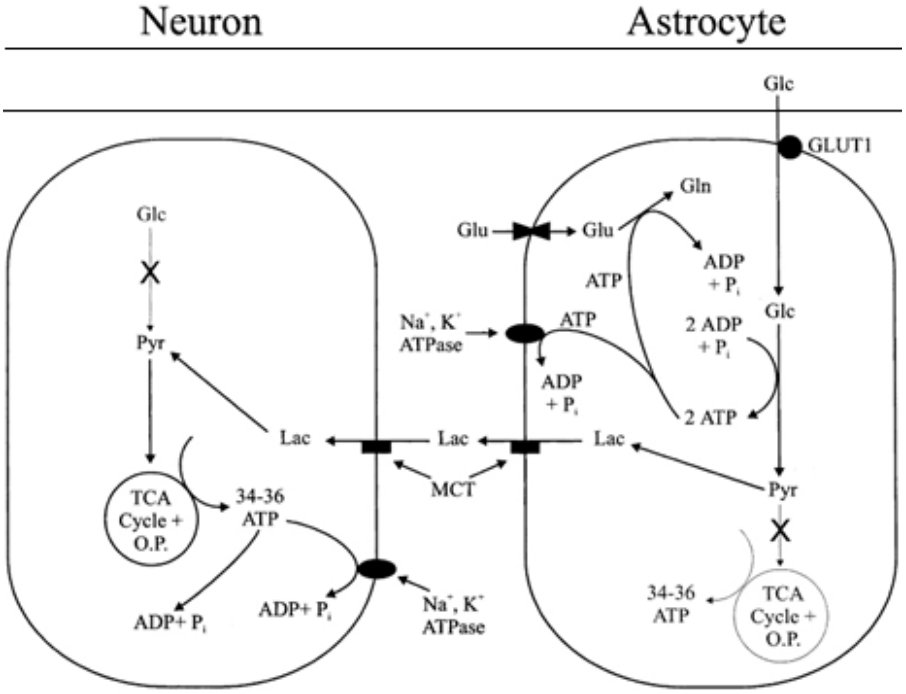

Figure 2. Schematic illustration of glucose metabolism during neural activity in neurons and astrocytes, according to the ANLSH. Adapted from Chih and Roberts, 2003

More recently, based on kinetic properties of the transporters of glucose and lactate and the concentrations of these metabolites in the various tissue compartments, Simpson et al. proposed that the neurons metabolize glucose to lactate and astrocytes use this lactate to fuel oxidative phosphorylation[6,11]. This hypothesis is called the neuron-to-astrocyte lactate shuttle hypothesis (NALSH).

The conventional theory of brain metabolism (figure 1) defends that in the case of increased metabolic demand after a neuron depolarization, both astrocytes and neurons oxidize glucose to meet their energetic demands, the production of lactate in this situation is atributed to the production of glycolitic products that exceeds the capacity of oxidative phosphorilation, and both astrocytes and neurons secrete those products to the bloodstream in the form of lactate[7].

As for the primary substrate of the brain as a whole, glucose is generally accepted as the metabolic substrate of the brain overall. The suitability of a substrate to act as the physiological fuel for the brain tissue may be evaluated by determining by

how efficiently the endothelial cells of BBB mediate its transport to the brain interstitial space. The endothelial cells of BBB transport glucose through glucose transporters (GLUT) at a maximum rate of 259.5 nmol/10^6 cell.min^{-1}. The GLUT have an Michaelis constant (K_m) of 8 mmol/L. Lactate is transported by the monocarboxylate transporters (MCT) of the endothelial cells at a rate of 10 nmol/10^6 cell.min^{-1} and a K_m for lactate[6] of 4 mmol/L. The low gradient of lactate across the blood brain barrier, coupled to the low lactate transport capacity of the endothelial cells, make lactate an ill-suited blood-borne metabolic substrate to the brain tissue as whole when compared to glucose[12].

The fact that glucose makes the better metabolic substrate in terms of availability and transport does not prove or disprove any of the aforementioned theories. NALSH and ANLSH each propose that a specific cell type is capable and responsible for the conversion of glucose to lactate, which serves as substrate to the other cell type.

Although the answer to the question of what is the primary substrate of the brain would be glucose, there is still no definite answer to what is the main metabolic substrate of neurons, what is the main substrate of astrocytes and if they change during periods of neural activity. At this point, the issue remains controversial, with frequent publications with contradictory and matching results to the ANLSH[6,11,13–15]. We aim to help shed some light in the issue with the respirometry approach.

1.1.2 Oxidative Phosphorylation

Oxidative phosphorylation is the process in which ATP is formed as a result of the transfer of electrons from the reduced form of nicotinamide adenine dinucleotide (NADH) and the reduced form of flavin adenine dinucleotide ($FADH_2$) to O_2 through a series of electron carriers that together make the electron transfer system (ETS) (figure 3). The oxidative phosphorylation pathway is the major source of ATP in aerobic organisms, as it yields an additional 26 molecules of ATP per glucose molecule as compared to the anaerobic fermentation of glucose, which yields 4 molecules of ATP per glucose molecule[16].

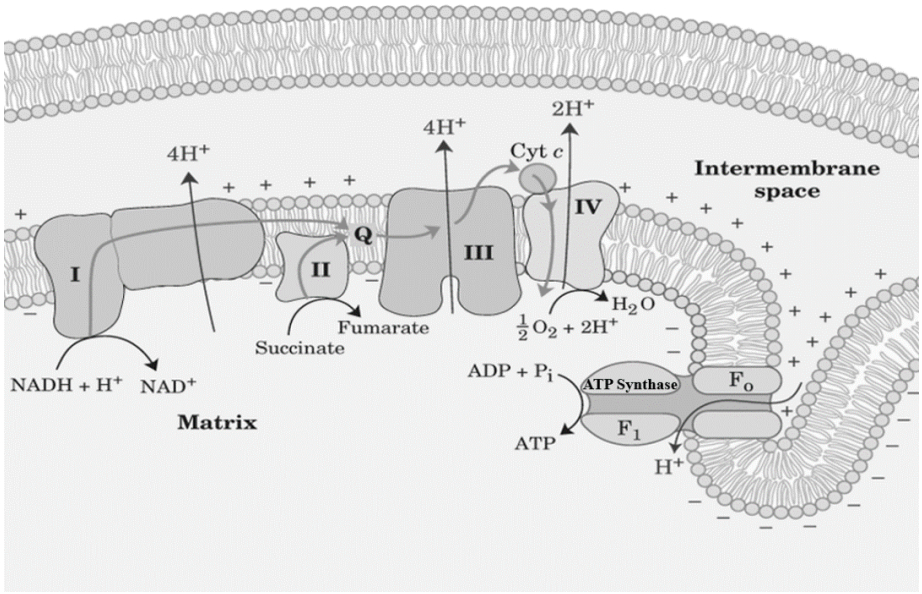

Figure 3. Oxidative Phosphorilation. Schematic representation of the ETC with complexes I, II, III and IV, ubiquitinol molecule (Q), cytochrome C (cyt C) and ATP synthase. Adapted from Nelson, Lehninger, and Cox, 2008.

The flow of electrons from NADH and $FADH_2$ to O_2 through a chain of protein complexes in the inner membrane of the mitochondria results in the pumping of protons to the intermembrane space of the mitochondria, forming a pH and electric gradient that favours the transport of protons to the mitochondrial matrix. The energy potential stored in the form of the proton electrochemical gradient is used by ATP synthase to catalyse the phosphorylation of ADP to ATP, at the cost of the transport of one proton to the mitochondrial lumen[17].

The electrons from NADH enter the chain in the NADH-Q reductase, also called complex I. Complex I consists of 34 polypeptide chains that together act as an electron carrier and proton pump. NADH is oxidized to its oxidized form (NAD^+) transferring two electrons to the complex, resulting in the pumping of four protons to the intermembrane space. The electrons are carried through a series of iron clusters in the complex I until they reach and reduce a molecule of ubiquitinone allocated in the inner membrane of the mitochondria. Complex I is inhibited by rotenone, amytal[18], myxothiazol and piericidin, property that are used in experiments of cell respirometry[19,20].

Another entryway for electrons in the ETS is succinate dehydrogenase or complex II. This complex catalyzes the oxidation of succinate to fumarate and transfers the electrons to reduce a molecule of ubiquitonone to ubiquitinol. It is the only enzyme of the ETS that also is also an enzyme of the tricarboxylic acid cycle (TCA). Unlike complexes I, III and IV, complex II is unable to pump protons to the intermembrane space. Inhibitors acting in this complex include malonate and thenoyltrifluoroacetone (TTFA)[16,21,22].

As both complexes reduce ubiquitinone to ubiquitinol, the electrons are then transferred from ubiquitinol to cytochrochrome c (cyt c) by an enzyme named cytochrome c reductase, also known as complex III. While the two electrons from ubiquitinol reduce cyt c, the complex pumps four protons to the intermembrane space. Antimycin A inhibits the oxidation of ubiquitin, preventing electron carrying and proton pumping by the complex III[17].

The last enzyme of the ETS is cytochrome c oxidase, or complex IV, which transfers the electrons from the cyt c to molecular O_2, reducing it to two water molecules. Complex IV also functions as a proton pump, pumping two protons per pair of electrons carried. The reduction of O_2 by complex IV is inhibited by cyanide, carbon monoxide, nitric oxide and hydrogen sulfide, all of which inhibit complex IV by binding to cytochrome a3 of the enzyme[17,23].

All the energy stored as a proton gradient formed by the oxidative phosphorylation enzymes is then used by ATP synthase to drive the phosphorylation of ADP to ATP. The ATP synthase can be inhibited by olygomycin and venturicidin[16].

Using polarographic O_2 sensors and the knowledge of substrates and inhibitors of the enzymes that are part of the ETS, it is possible to design respirometry experiments that give insight about the properties of populations of mitochondria.

1.1.3 Nitric Oxide

Nitric Oxide ($^{\bullet}NO$) is a non-polar gas and a free radical. As a free-radical it reacts rapidly with other molecules, especially with other free-radicals and transition metals like

those found in heme groups[24]. Being a non-polar species it can freely diffuse through membranes, in fact the diffusion of •NO through lipid membranes is 1.4 times greater than O_2. This means that nitric oxide can diffuse intercellular distances until it reacts with its targets in the surroundings cells[24].

The enzymes capable of generating •NO are called the nitric oxide synthases (NOS). They catalyse the oxidation of L-arginine and O_2 to •NO molecule and L-citrulline, oxidizing a molecule of NADPH in the process (figure 4).

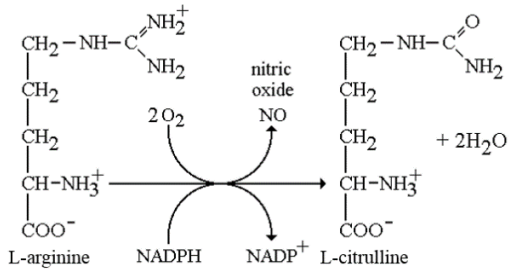

Figure 4. Reaction catalyzed by NOS. In the presence of O_2 and NADPH, NOS converts L-arginine to L-citrulline and •NO.

Three isoforms of NOS can be found in mammal cells, namely the neuronal nitric oxide synthase (nNOS or NOSI), the inducible nitric oxide synthase (iNOS or NOSII) and the endothelial nitric oxide synthase (eNOS or NOSIII). Isoforms nNOS and eNOS, also called constitutive nitric oxide synthases (cNOS), depend on calcium for activation. In contrast, iNOS activation is independent of calcium and it is only expressed during an immune response[25].

All three isoforms of NOS can be found in the mammal brain. nNOS is highly expressed in neurons and is calcium dependent, since activation requires the binding of calcium-bound calmodulin. The nNOS contains a PDZ domain at the N-terminus that anchors the protein to the postsynaptic density protein-95 (PSD-95), which indicates that nNOS is located at the postsynaptic density. This subcellular location implies that nNOS is at the site of calcium entry into the neuron upon synaptic stimulus, allowing a thight coipling between synaptic transmission and neuronal •NO production[26].

Glutamatergic transmission stimulates the production of •NO through the activation of NMDA receptors, one of the two ionotropic glutamate receptors. NMDA receptors are permeable to calcium ions and, like nNOS, they are associated to PSD95, resulting in

the co-location of both NMDA and nNOS. So, NMDA receptors lead to the entry of calcium to the cell, which binds to calmodulin to activate nNOS[26].

The iNOS can be expressed in glial cells in response to an inflammation stimulus, which results in the production of pro-inflammatory transcription factors like interferon regulatory factor-1 (IRF-1) and the nuclear factor kappa-light-chain-enhancer of activated B cells (NF-κB). The iNOS isoform is independent of calcium, as it is permanently bound to calmodulin[27].

The eNOS is expressed in endothelial cells, they are present in the blood vessels of the brain. The myristoylation and palmytoylation of eNOS allows binding to calveolin-1 which prevents eNOS activation. The unbinding from caveolin-1 requires the presence of calcium, and once unattached, the activation of eNOS requires both the phosphorylation by phosphatidylinositol 3-kinase (PI3K) and the binding of calmadulin[27].

One of the main cellular targets of $^{\bullet}NO$ is the soluble guanylyl cyclase (sGC), which is activated when bound to $^{\bullet}NO$, producing cyclic guanosine monophosphate (cGMP). cGMP leads to activation of protein kinases such as protein kinase G (PKG). $^{\bullet}NO$ is also capable inhibiting O_2 consumption by binding reversibly to the complex IV[28].

$^{\bullet}NO$ can also modulate O_2 consumption by binding and reversibly inhibiting complex IV. It binds to complex IV in the O_2 binding site, in competing with O_2.

1.2 RESPIROMETRY TECHNIQUES

The term respirometry describes two distinct techniques, whole-animal respirometry and mitochondrial (or cell) respirometry, both of which aim at gaining insights on energetic metabolism through the measurement of O_2 consumption.

In the whole-animal respirometry, the animal is kept alive and breathing to a respirometer (figure 6) that measures the volume of O_2 inhaled and the carbon dioxide exhaled. The ratio between carbon dioxide exhaled per O_2 inhaled gives the respiratory coefficient, which is 1.0 for carbohydrates but less for lipids and proteins as energy source.

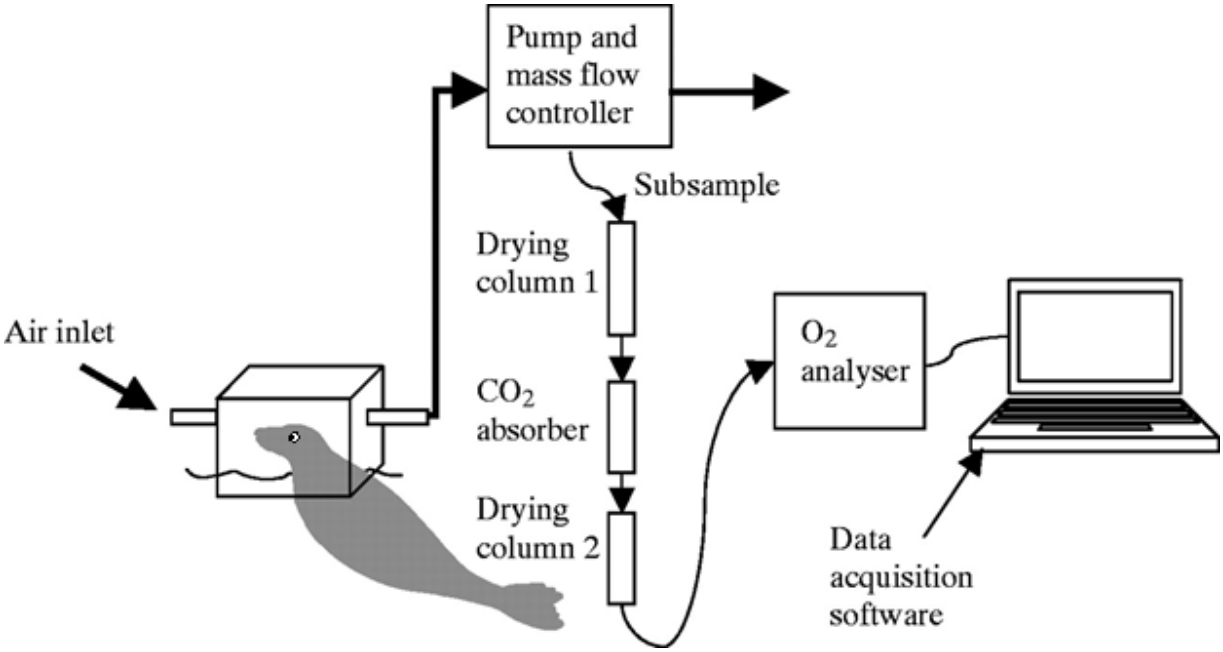

Figure 5. Schematic representation of a whole-animal respirometry system. The arrows show the direction of air-flow through the system. Adapted from Sparling and Fedak, 2004

The first measurements of cell respiration were made by the Nobel-prize laureate Otto Heinrich Warburg using the so-called "Warburg apparatus" (figure 7). Warburg used a manometric approach to quantify O_2 consumption in tissue slices. The carbon dioxide was absorbed by a solution of potassium hydroxide in a well in the middle of the chamber, making the consumption of O_2 the sole contributor for barometric decrease of the chamber's pressure. The decrease of the chambers pressure is then measured using a manometer[30,31].

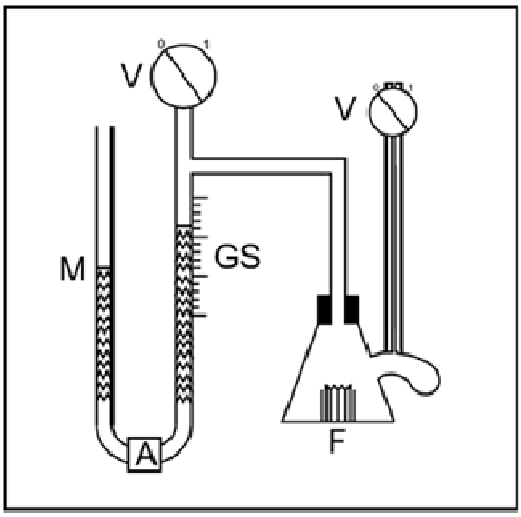

Figure 6. Schematic representation of the Warburg manometric respirometer. A manometer (M) measures the drop in pressure caused by O_2 consumption in the flask (F). The valves (V) are closed during readings. Graduated Scale (GS). Fluted filter paper soaked in KOH solution is placed in a center well in the flask and acts as a CO_2 absorbent. Adapted from Lighton, 2008

Nowadays most cell (and mitochondrial) respirometry studies use polarographic O_2 electrodes, also called Clark-type electrodes, invented by Leland Clark. The polarographic O_2 electrode consists of an Ag/AgCl anode and a platinum or gold cathode. These two components are connected by an electrolyte solution (usually KCl) and separated from the sample by an O_2 permeable membrane. In the case of an Ag/AgCl reference electrode, the applied potential required for O_2 reduction varies from -0.8 to -0.6 V[30,32,33]. The reactions taking place are:

$$O_2 + 4H^+ + 4e^- \rightarrow 2H_2O \qquad \text{(Eq. 1)}$$

and,

$$4Ag + 4Cl \rightarrow 4AgCl + 4e^- \qquad \text{(Eq. 2)}$$

1.2.1 High-Resolution Respirometry

The term high-resolution respirometry was coined by Erich Gnaiger to describe the O_2 measurements obtained by using the OROBOROS Oxygraph O2k in conjunction with the use of the DatLAB software, both products of the company Oroboros Instruments. The OROBOROS Oxygraph O2k uses a Clark-type polarographic O_2 sensor consisting of a gold cathode and an Ag/AgCl anode connect by a KCl electrolyte solution and separated from the sample by an O_2 permeable flurinated ethylene propylene (FEP) membrane. The electrode is polarized to -0.8 V, allowing the electrochemical reduction of the O_2 that diffuses across the FEP membrane. High-resolution respirometry owes its name to being capable of detecting a respiratory flux of 1 pmol.s^{-1}.cm^{-3} and having a limit of detection for O_2 of 0.005 µM.

1.2.2 Respirometry of Intact Cells

As its name indicates, respirometry of intact cells is an experimental procedure using non-permeabilized cells from cell cultures, biopsies or, in the case of this thesis, rat hippocampal slices. Respirometry of intact cells differs from respirometry of isolated mitochondria due to many factors, the main one is the presence of the cellular membrane, which blocks or delays the diffusion of many mitochondrial inhibitors and

most substrates used with isolated mitochondria. The second is the presence of the cellular machinery, organelles, enzymes and nucleus, which are not accounted for in isolated mitochondria and which may confer specific properties to the biological preparation. For example, one may observe an increase in O_2 consumption upon glutamate titration in both hippocampal slices and breast cancer cells, however the increase in hippocampal slices is due to an excitatory effect by glutamate that increases the metabolic rate while in breast cancer cells, glutamate acts as an anaplerotic substrate to the TCA cycle, serving as a fuel to oxidative phosphorylation[34].

The experiments of cell (and mitochondrial) respirometry consist in the measurement and manipulation of the respiratory O_2 flux, also called oxygen consumption rate (OCR). The OCR can be modulated by a myriad of substrates or inhibitors for the complexes.

Flux control ratios (FCR) express respiratory control independent of mitochondrial content and cell size. FCR's are OCR's in the presence of different inhibitors and substrates normalized for maximum and minimum flux corresponding respectively to the values of 1.0 and 0.0. The OCRs in intact cell respirometry are normalized to FCRs using the OCR of the uncoupled mitochondria as the maximum flux attainable by the ETS (with a value of 1) and the OCR after the complete inhibition of ETS as the minimum flux (with a value of 0)[32].

The uncoupled state is induced by adding a mitochondrial uncoupler like varbonyl cyanide m-chloro phenyl hydrazone (CCCP), 2,4-dinitrophenol (DNP), carbonyl cyanide 4-(trifluoromethoxy)phenylhydrazone (FCCP) or 4,5,6,7-tetrachloro-2-trifluoromethyl-benzimidazole (TTFB). These drugs are ionophores that dissipate the proton gradient between the intermembrane space of the mitochondria and the mitochondrial matrix[16]. Loss of this gradient leads proton pumps (complex I, III and IV) to catalyse the reactions at maximum capacity, effectively resulting in maximum O_2 reduction as long as substrates are available.

Complete inhibition of ETC (the minimum flux) can be attained in intact cells by using rotenone, antimycin A or cyanide. After the titration of these drugs it's possible to

still measure an, albeit lower, OCR, attributed to lipid peroxidation or residual atmospheric diffusion[32].

One FCR obtained from intact cell respirometry is the ROUTINE respiration, which is the basal respiration supported by exogenous substrates supplemented in the medium. This FCR can be influenced by the coupled state of the mitochondria, the energy demand of the cells or the capacity of the cells to metabolize the supplemented substrates[35,36].

Another FCR determined for intact cells is the LEAK state, which reflects the rate of O_2 consumption non-coupled to ADP phosphorylation. The O_2 consumed in this state is used to compensate the dissipation of the proton gradient and can be induced by inhibitors for the ATP synthase or the ATP-ADP translocase[37]. A high LEAK state may mean that the mitochondria are not in perfect conditions, as it may indicate a compromised mitochondrial membrane that is allowing the dissipation of the proton gradient[32].

The Respiratory Viability Index (RVI) is an FCR that allows the viability in a specific biological preparation to be assessed. Complex II is inactivated in intact cells after inhibition of complex I, as succinate production is halted because NADH cannot be recycled. Plasma membrane is impermeable to succinate, so the addition of exogenous succinate to intact cells has no effect on their O_2 consumption. Yet succinate added to cells with a compromised membrane will be able to reach mitochondrial complex II and donate electrons. In an experiment of intact cell respirometry, the OCR obtained from succinate titration is only due to compromised cells respiration.

The RVI was already attested by comparison with the results obtained from a CASY 1 Cell Counter and Analyser System (Schärfe System) which also evaluates cell viability, the results of cell viability obtained from the CASY equipment matches the results for the RVI[19].

The ratio between the uncoupled state and the inhibited state of the ETS is called the RESIDUAL ratio, and its value is a function of O_2 consumption not attributed to mitochondrial respiration[32].

1.3 THE HIPPOCAMPUS

The hippocampus is a structure of the temporal medial lobe. It is divided in six major regions, which are connected by a unidirectional neuronal pathway along the called proximo-distal axis. These six regions are organized along the axis in the following order: dentate gyrus, cornu ammonis (CA) fields, subiculum, presubiculum, parasubiculum and entorhinal cortex[38]. There is additional connectivity between the six regions that doesn't follow the proximal-distal axis, but the majority of neuronal connections inside the hippocampus, including those along the axis, still follow a transverse orientation (figure 8).

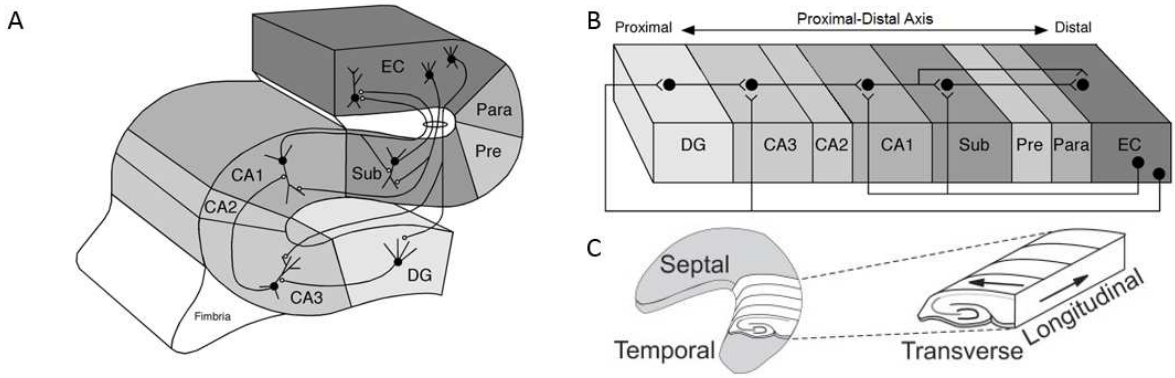

Figure 7. Hippocampus organization. (A) Major regions and subregions of the hippocampus are the dentate gyrus (DG), CA3, CA1, CA3, subiculum (Sub), presubiculum (Pre), parasubiculum (Para) and entorhino cortex (EC). (B) Disposition of the hippocampus regions along the proximal-distal axis with the corresponding projections connecting the regions. (C) Three-dimensional representation of the hippocampus illustrating the orientation of the transverse and longitudinal axis as well as the septal and temporal poles. Adapted from Gloveli et al., 2005 and Andersen et al., 2006.

The CA field is divided in three subregions they are, along the proximal-distal axis, CA3, CA2 and CA1. These three subregions are structured with defined layers with different cell composition, namely the alveus, stratum oriens, stratum pyramidal and the stratum stratum lacunosum-moleculare (figure 9). The cell bodies of the pyramidal neurons can be found in the stratum pyramidal, alongside many cell bodies of interneurons. Astrocytes are rare in stratum pyramidal but are common in the other layers of the CA fields [40].

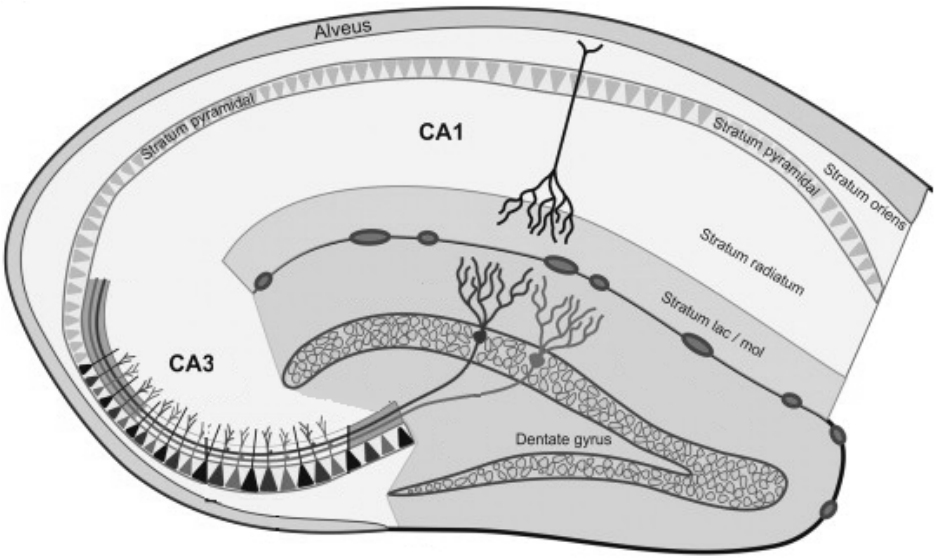

Figure 8. Hippocampus layered structure. Schematic representation of the layer structure of the CA fields, including the alveus, stratum oriens, stratum radiatum and stratum lacunosum-moleculare. Adapted from Nagy, 2012.

2 OBJECTIVES

The major goal of this study was do investigate the ability of lactate to act as an alternative fuel to sustain cellular respiration, in both basal conditions and under increased neuronal activity in hippocampal slice, as well as appraise a putative shift towards aerobic glycolysis evoked by increased neuronal activity. To achieve this goal we employed high-resolution respirometry to evaluate whole cell respiration in slices under distinct metabolic states.

To this purpose, the specific goals were:

i) Establish and validate an appropriate protocol to evaluate acute rat hippocampal slices without compromising cytoarchitectural organization and neuronal circuitry using the OROBOROS Oxygraph-O2k to measure OCR's;

ii) Test if brain activation induced by glutamate increased O_2 consumption due to its effect on energy demand of the hippocampal cells or decreased O_2 consumption of the hippocampal cells due to the induction of aerobic glycolysis in the astrocytes of the tissue;

iii) Compare lactate and glucose as oxidative substrates in both basal respiration and under glutamate-induced hippocampal activation;

iv) Measure the effects of •NO on the acute rat hippocampal slice respiration due to a possible role on oxidative metabolism regulation.

3 MATERIALS AND METHODS

3.1 CHEMICALS AND BIOCHEMICALS

The media for all experiments using hippocampal slices was aCSF. The base composition was (in mM): 120 NaCl, 3 KCl, 26 $NaHCO_3$, 1.5 NaH_2PO_4, 1.5 $CaCl_2$ and 1 $MgCl_2$. Depending on the specifications of the experiments, other components were added.

For preparation and recovery of the 200 µm thick slices the base solution was supplemented with 10 mM glucose, 0.2 mM ascorbate and 1 mM glutathione, continually bubbled with humidified carbox (95% O_2/5% CO_2) for oxygenation and pH buffering.

The 100 µm thick slices were prepared and incubated in the base solution plus 0.2 mM ascorbate, 1 mM glutathione, 20 mM HEPES and 10 mM or 20 mM glucose depending on the experiment, at atmospheric O_2 concentration.

The O_2 recordings were performed in a solution composed of the base solution plus (in mM) 20 HEPES and 10 glucose, 20 glucose or 20 sodium lactate depending on the experiment.

Fatty-acid free BSA and NaCl were from Merck Milipore. All other reagents were from Sigma-Aldrich.

3.2 LAB-MADE EQUIPMENT

To maintain the histological and network integrity of the hippocampal slices during respirometry experiments, it was necessary to develop a device, hereby referred to as floater, made out of materials available in the lab. To build a floater, we used two 5 ml pipette tips made of polypropylene plastic and cut a 25 mm diameter circle of nylon mesh (figure 10). One of the pipette tips was dovetailed in the other and a segment of 50 mm was cut in the overlap between the two, making the inner ring and the outer ring. The nylon mesh circle was then pinched between the outer ring and the inner ring. This sole piece acted as a support for the slices in the chamber of the

OROBOROS.

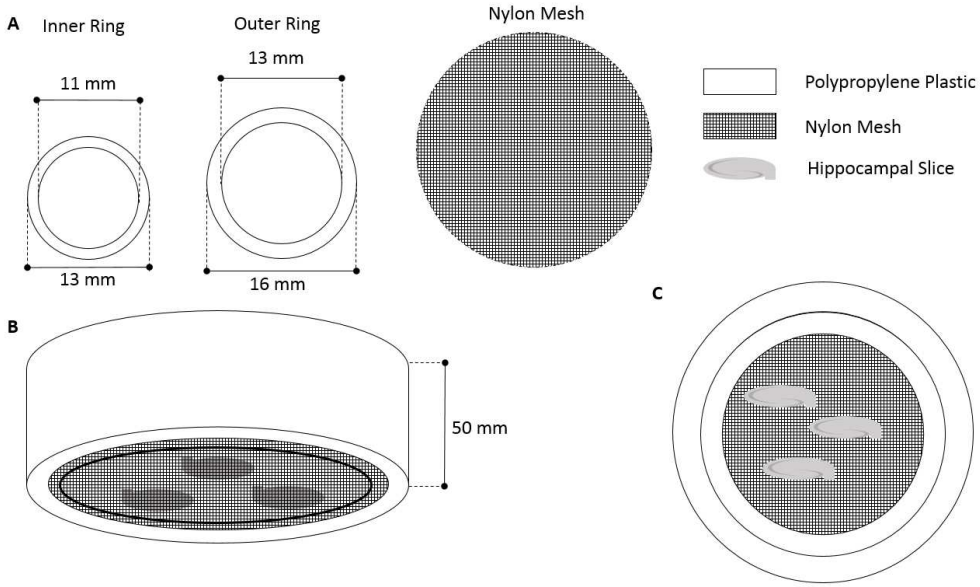

Figure 9. Components and dimensions of the floater device. (A) Individual components and respective dimensions of the floater, the inner ring, the outer ring and the nylon mesh. (B) and (C) Different perspectives of the mounted floater.

3.3 ANIMALS AND SLICE PREPARATION

Male Wistar rats with ages from 7 to 14 weeks were anesthetized with halothane and then euthanized by cervical displacement. The brain was rapidly removed and placed in ice-cold modified aCSF. After dissection, the hippocampi were sliced in the transversal orientation with a thickness of 200 µm or 100 µm using a Vibroslice NVS2M1 (World Precision Instruments) while submerged in ice-cold modified aCSF bubbled with carbox. The slices were placed in a pre-incubation chamber and allowed to recover for at least 1.5 hours at room temperature.

3.4 SLICE RESPIROMETRY

Measurement of O_2 consumption from hippocampal slices were made using an Oroboros Oxygraph-O2k (Oroboros Instruments). The Oxygraph-O2k (figure 11) was set to maintain a 32ºC temperature, at the maximum stirring speed of 900 rpm and the gain 1.

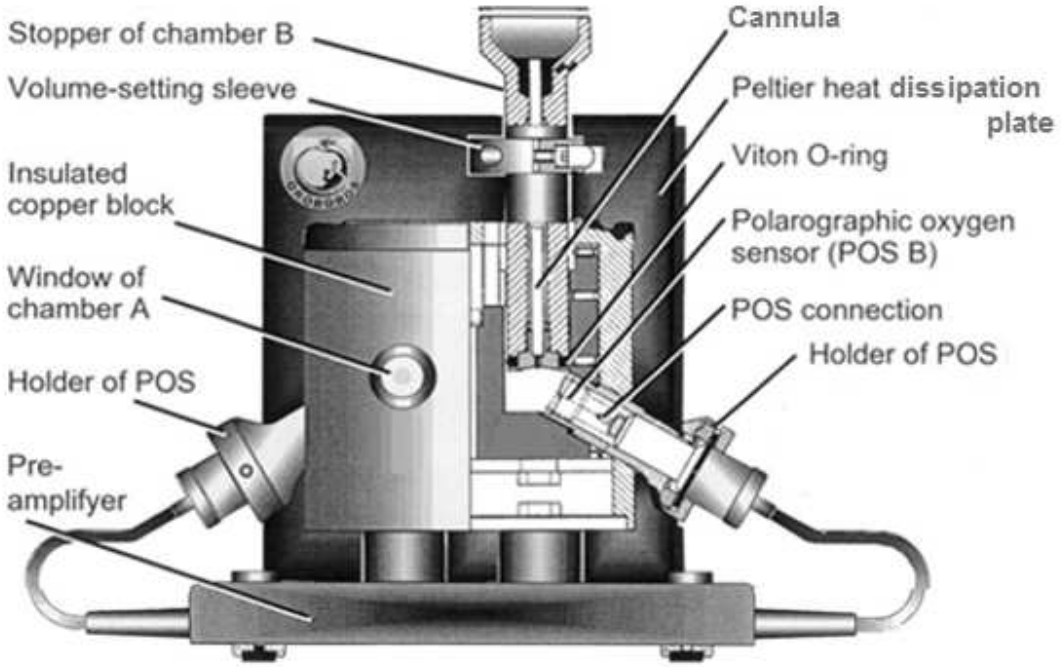

Figure 10. **The Oroboros Oxygraph O2k**. A two chamber system with two polarographic O_2 sensors. Adapted from Gnaiger 2001.

A floater was made to keep the network integrity and tissue organization of the hippocampal slices. The function of these device was to float inside the chamber and support the slices using a nylon mesh, keeping them in the middle of the chamber away from the magnetic stirrer, thus avoiding mechanical damage to the tissue.

For each experiment we added 3 hippocampal brain slices to the OROBOROS chamber. For the respirometry of 200 µm slices, the medium in the chamber was previously bubbled with carbox. After the O_2 concentrations stabilized, the slices were placed inside the chamber, atop the nylon mesh. The chamber was quickly closed to avoid O_2 diffusion between the medium and the atmosphere. The 100 µm slices didn't require prior oxygenation of the medium.

To facilitate drug delivery across the cell membrane, fatty-acid free bovine serum albumin (BSA), in a concentration of 5 mg/ml, was added to the chamber immediately after closing it.

3.5 MEASUREMENT OF FLUX CONTROL RATIOS (FCR)

The values for the FCR's were calculated from the OCR's measured after the titration of a respiration modulator or a series of modulators (figure 12). To obtain the value of a FCR we needed to obtain the OCR in the uncoupled state (E'), to induce this slope, we titrated 30 µm FCCP and waited for the slope to stabilize, the value of the OCR at that point was E'. To further ensure that the ETS was working at maximum capacity during this state, five minutes before the titration of FCCP we titrated 5 mM pyruvate, this ensures that enough substrate reaches the mitochondria to fuel this state.

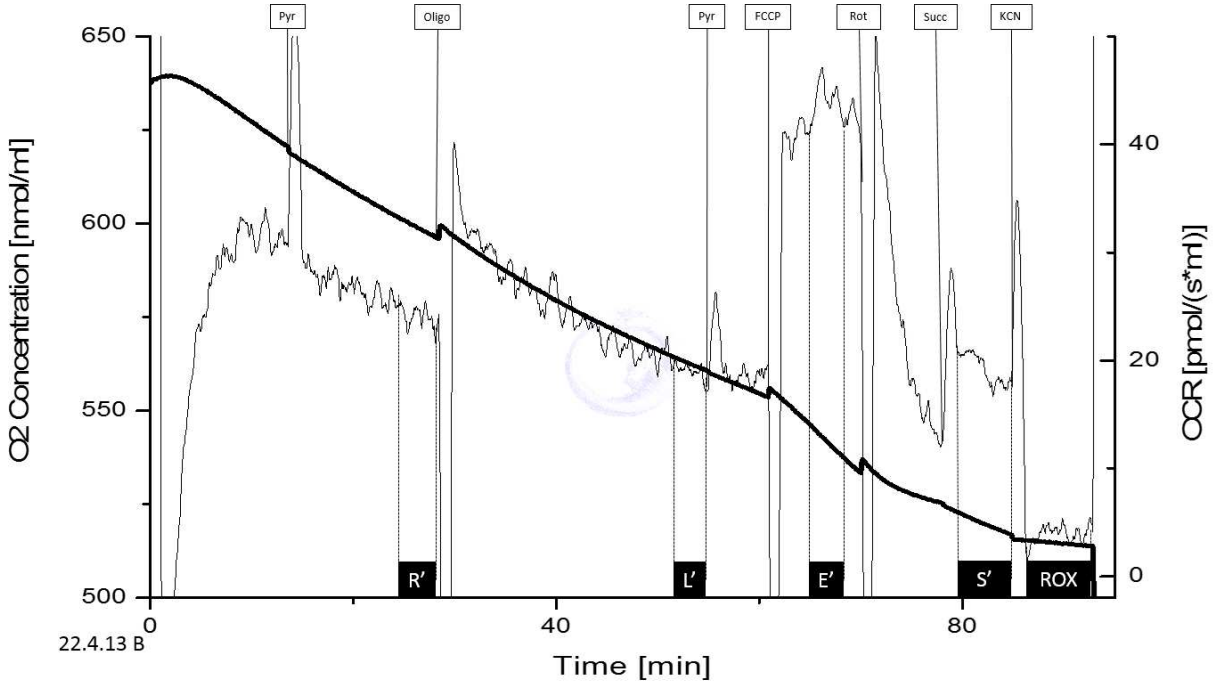

Figure 11 Typical experiment of high-resolution respirometry of acute rat hippocampal slices. The R' is the basal OCR fuelled by the metabolic substrates in the medium. The L' represents the OCR obtained for respiration non-coupled to ATP phosphorylation. The E' is the OCR obtained when the ETS is functioning at its maximum capacity or in an uncoupled state. The S' represents the OCR obtained for complex II-mediated respiration of the mitochondria from non-viable tissue. And the ROX is the residual OCR.

To calculate the FCR's we also needed the value of the slope for when respiration is fully inhibited (ROX). As such, our last modulator used in the experiments was 5 mM KCN, and the OCR after the titration is the value for ROX.

The ROUTINE state was calculated using equation 3. The value for R' was obtained by waiting at least fifteen minutes for the slope to stabilize after the closing of

the chamber prior to the addition of other modulators. The value of the slope at this point was the R' value.

$$\mathrm{ROUTINE} = \frac{R' - \mathrm{ROX}}{E' - \mathrm{ROX}} \qquad \text{(Eq. 3)}$$

The LEAK state was calculated by inhibiting the O_2 consumption associated with the production of ATP using oligomycin to inhibit ATP synthase. The OCR after the injection of oligomycin would be the L' value.

$$\mathrm{LEAK} = \frac{L' - \mathrm{ROX}}{E' - \mathrm{ROX}} \qquad \text{(Eq. 4)}$$

The values for RVI were obtained by the inhibition of complex I with rotenone after the induction of the uncoupled state, after which respiration was titrated with succinate. The slope at this point (S') was used to calculate the RVI.

$$\mathrm{RVI} = \frac{S' - \mathrm{ROX}}{E' - \mathrm{ROX}} \qquad \text{(Eq. 5)}$$

The ratio between the inhibited state (ROX) and the uncoupled state determines the RESIDUAL O_2 consumption.

$$\mathrm{RESIDUAL} = \frac{\mathrm{ROX}}{E'} \qquad \text{(Eq. 6)}$$

3.6 DATA ANALYSIS

OCRs were acquired using the DatLAB version 4 (Oroboros Instruments). Numerical values are presented as means ± SD and graphs as means ± SEM. Statistical significance of the difference between two values was evaluated by unpaired Student t-test.

4 RESULTS AND DISCUSSION

4.1 RESPIROMETRY RECORDING AT HIGH OXYGEN TENSION

The most common thicknesses used for the preparation of acute brain slices are 400 µm and 300 µm. These thicknesses allow optimal diffusion of O_2 in the tissue, allowing a physiological concentration of O_2 in the tissue core to be achieved when bathed in solutions oxygenated with carbox[42], which maintains a constant concentration of approximately 1000 nmol/ml of O_2 at 25º C.

The medium we used for the experiments is bubbled with carbox prior to the measurements but between the removal of the carbox and the closing of the chamber, the O_2 concentrations drops dramatically and as the experiment continues, the O_2 concentration inside the chamber gradually decreases, under these conditions the centre of the 400 µm and 300 µm thick slices tend to become hypoxic. For these reasons we opted to use 200 µm thick hippocampal slices, expecting the normoxic conditions at the core of the slice to maintain even at the end of the experiment.

By using 200 µm thick slices, we were able to obtain FCR's for the ROUTINE state and the RVI (figure 13), but had difficulty obtaining results for the LEAK state.

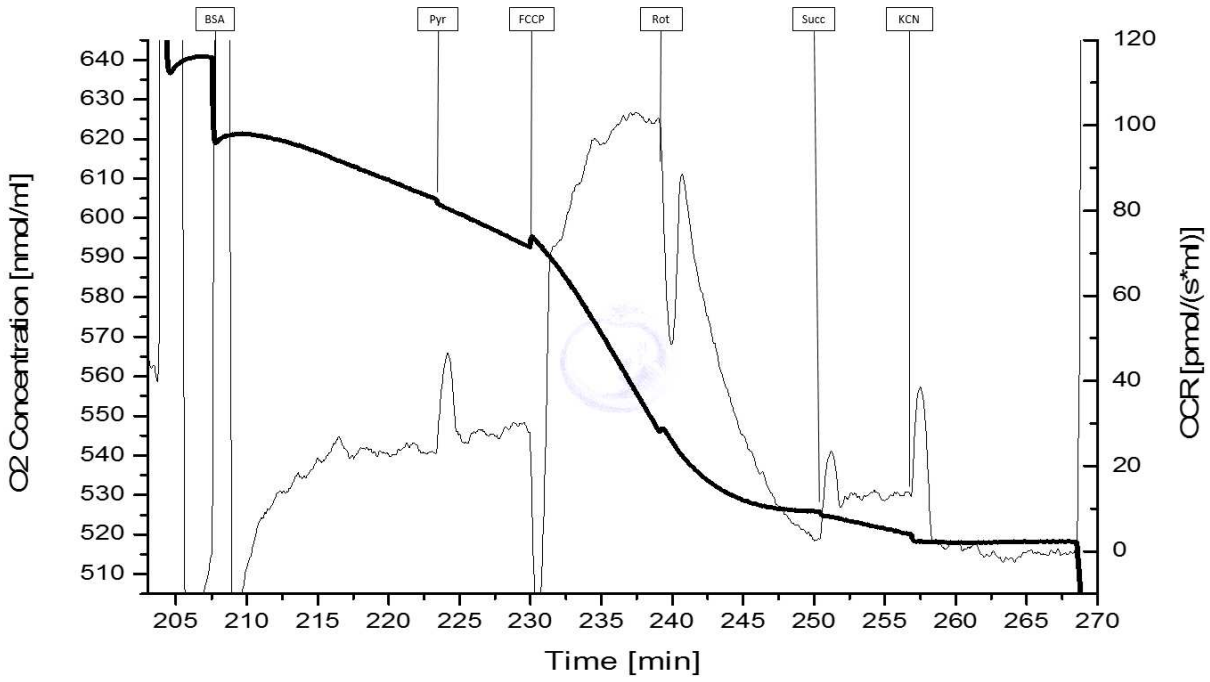

Figure 12. Respirometry recordings in high O_2 concentrations of an 200 µm acute hippocampal slice in a medium containing glucose (20 mM). The thick line is O_2 concentration (——) and the thin is line is the OCR (——). Successive titrations of 5 mg/ml fatty-acid free BSA, 5 mM pyruvate (Pyr), 30 µm FCCP, 5 µm rotenone (Rot), 5 mM succinate (Succ) and 5 mM KCN.

4.1.1 Measurement of the LEAK state

In order to validate our experimental approach and compare results with those published previously for high-resolution respirometry in intact cells, values for ROUTINE, LEAK and RESIDUAL FCR were determined. With regard to the LEAK state (O_2 consumption rate not associated to ADP phosphorylation), we are unable to observe and measure an effect of oligomycin on respiration in hippocampal slices (figure 14).

The lack of observable or measurable effect of oligomycin on the O_2 consumption may be due to the adsorption oligomycin to the polypropylene plastic of the floater. There is a correlation between high partition coefficient and polypropylene plastic adsorption[43], the partition coefficient estimated for oligomycin is 6.52, which is the highest among the drugs used in these experiments (the partition coefficient for FCCP and rotenone are 3.68 and 4.65 respectively; the partition coefficient was predicated using the software ADC\Log P[44]).

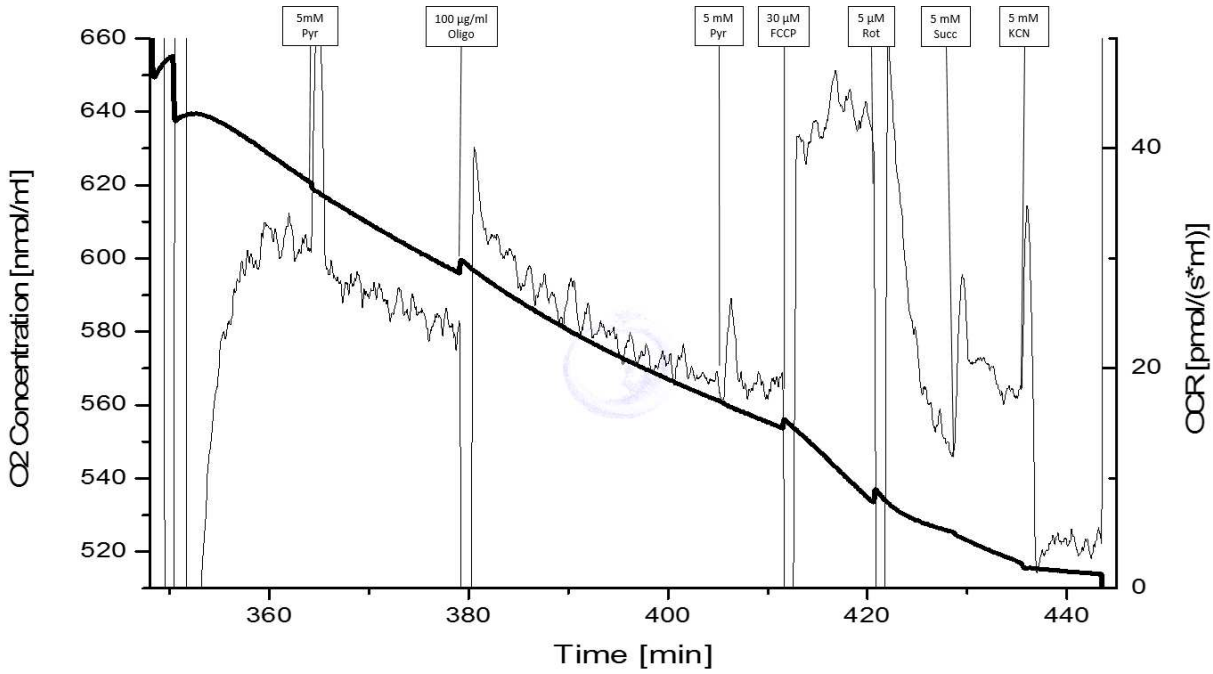

Figure 13. Effect of high concentration oligomycin (100 µm/mL) on cell respiration. The thick line is O_2 concentration (——) and the thin is line is the OCR (——). The recording were made at high O_2 concentration using 200 µm acute hippocampal slices. The following modulators were add in in the following order: 5 mg/ml of fatty-acid free BSA, 100 µg/ml of oligomycin (Oligo), 5 mM pyruvate (Pyr), 30 µm FCCP, 5 µm rotenone (Rot), 5 mM succinate and (Succ) and 5 mM KCN.

4.1.2 Effect of nitric oxide on the oxygen consumption rate

Nitric oxide (•NO) is an endogenous regulator of mitochondrial respiration. It competes with O_2 for binding to cytochrome c oxidase and can reversibly inhibit O_2 consumption[45]. This has been demonstrated to occur in simpler biological preparations, such as isolated mitochondria[46], synaptosomes[47] and intact cells[48], but has not been demonstrated to occur in a complex biological media, where cytoarchitectural and neuronal circuitry remain intact and functional, as is the case with hippocampal slices.

As shown in figure 15, under these particular experimental conditions, even very high concentrations of •NO added to the media had no observable inhibitory on the OCR of 200 um hippocampal slices. The main reason for this observation is the high O_2 concentration present in the recording chamber.

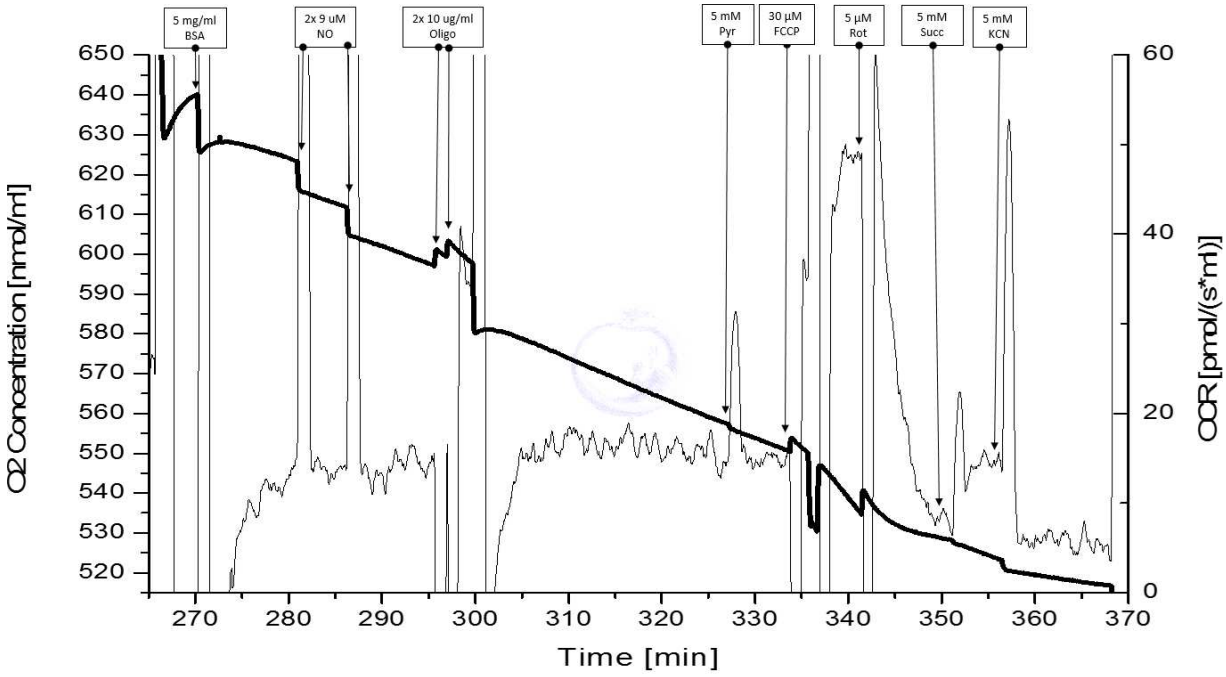

Figure 14. Effects of nitric oxide on respiratory rates under high O_2 concentrations in 200 µm thick hippocampal slices. The thick line is O_2 concentration (——) and the thin is line is the OCR (——). Successive titrations of 5 mg/ml fatty-acid free BSA, two additions of 9 µm •NO, 5 mM pyruvate (Pyr), 30 µm FCCP, 5 µm rotenone (Rot), 5 mM succinate (Succ) and 5 mM KCN.

In an aerobic aqueous solution, •NO reacts with O_2 to yield dioxide nitrogen, which is then rapidly hydrolyzed to nitrite [49,50]. This reaction follows the overall equation:

$$4NO^{\bullet} + 2O_2 + 2H_2O \rightarrow 2NO_2 + 2NO^{\bullet} + 2H_2O \rightarrow 4H^+ + 4NO_2^- \quad \text{(Eq. 7)}$$

We propose that due to the high concentrations of O2 in the chamber, which ranged from 500 nmol/ml to 1000 nmol/ml, the •NO added to the recording chamber reacts with the O_2, yielding nitrite, before reaching the hippocampal slices, resulting in a *de facto* concentration of •NO in the chamber much lower than expected.

4.2 RESPIROMETRY RECORDING AT LOW OXYGEN TENSION

Due to the above mentioned difficulties associated with the evaluation of •NO in hippocampal slice respirometry and taking in account the reactivity of •NO with the high

concentration of O_2 in the media, the experimental approach was adapted to perform high-resolution respirometry of rat hippocampal slices at lower O_2 concentrations.

At low O_2 concentration no changes in OCR were observed when using 200 µm slices upon the addition of FCCP, rotenone or KCN. This was not unexpected, since unadequate oxygenation of tissue is possible at lower O_2 concentrations.

To circumvent this problem, thinner slices were prepared. By preparing 100 µm thick slices we were able to measure and compare the values of FCR's previously measured in the 200 µm thick slices under high O_2 concentrations (figure 16).

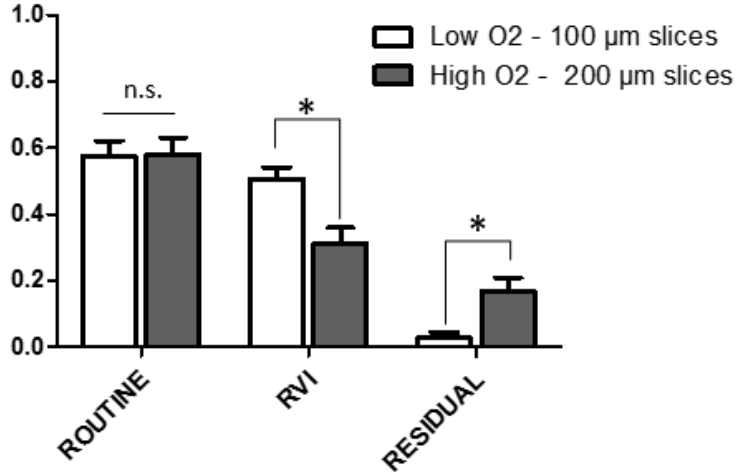

Figure 15. Comparison of the FCR values obtained for experiments with low O_2 concentration and 100 µm hippocampal slices (n=6) and the experiments at high O_2 concentrations and 200 µm slices (n=8). There was a statistically significant difference between the RESIDUAL and RVI ratios between the experiment settings but not for the ROUTINE state (p=0.939). * p<0.05.

The RVI value indicates the proportion of mitochondria from cells with a compromised cellular membrane. The differences in RVI observed between the 2 types of slices can be attributed to an increase in the ratio of dead/healthy cells in 100 µm slices versus 200 µm slices. As stated above, during the process of cutting of the hippocampus with the Vibroslice it is estimated that the acute slices obtained have a 10 µm layer of dead and/or damaged cells on each side of the slice[51]. In a slice with 100 µm thickness this dead layer would compromise 20% of the slice, while in a 200 µm thick slice it corresponds to 10%.

The decrease in the RESIDUAL FCR is justifiable by the lower instrumental background oxygen flux associated with O_2 concentration inside the chamber, which is closer to the atmospheric concentration in these experiments.

As for the ROUTINE state, there was not a significant difference between the low and high O_2 concentration experiments, which indicates that, although the proportion of viable cells is lower in 100 µm slices, the viable cells in both slice thicknesses have similar basal O_2 consumption rates when comparing to their maximum capacity.

4.2.1 Effect of nitric oxide on oxygen consumption rate

Under low O_2 concentrations we expect nitric oxide to keep in solution much longer than under high O_2. As shown in figure 17, addition of •NO to the recording chamber decreased OCR in hippocampal slices. Five minutes after the addition of the addition of 1.8 µM nitric oxide we observed a decrease of 15.6 ± 5 % compared to maximum flux and an additional 23.5 ± 0.4 % decrease after the addition of 18 µM of nitric

The fact that inhibition of cell respiration by nitric oxide was not reversed by the time period of 20 minutes has two plausible explanations: irreversible inhibition of the mitochondrial complexes due to •NO derivatives[52], or the lack of nitric oxide scavengers in preparation, such as haemoglobin, meaning that the *de facto* nitric oxide concentration in the solution was kept high[24].

It was reported that concentrations of 1 µM •NO in an isolated mitochondria preparation could yield a high enough concentration of peroxynitrite to partially inhibited complex I irreversibly [53]. Also in isolated mitochondria, a concentration of 5 µM •NO was shown to be able to partially irreversibly inhibit complex II[54].

Comparing the results for •NO and the RESIDUAL respiration for 100 and 200 µm slices it seems that the 100 µm at low O_2 concentration is the better experimental approach. The values for the ROUTINE state are maintained between the two approaches, but the lower O_2 concentrations allows for a chemistry closer to the physiological setting, as we can see from the results from •NO titration, and a lower instrumental background O_2 diffusion from the system. It seems the lower ratio of viable-to-unviable cells of the 100 µm slices doesn't affect the values of the respiratory states.

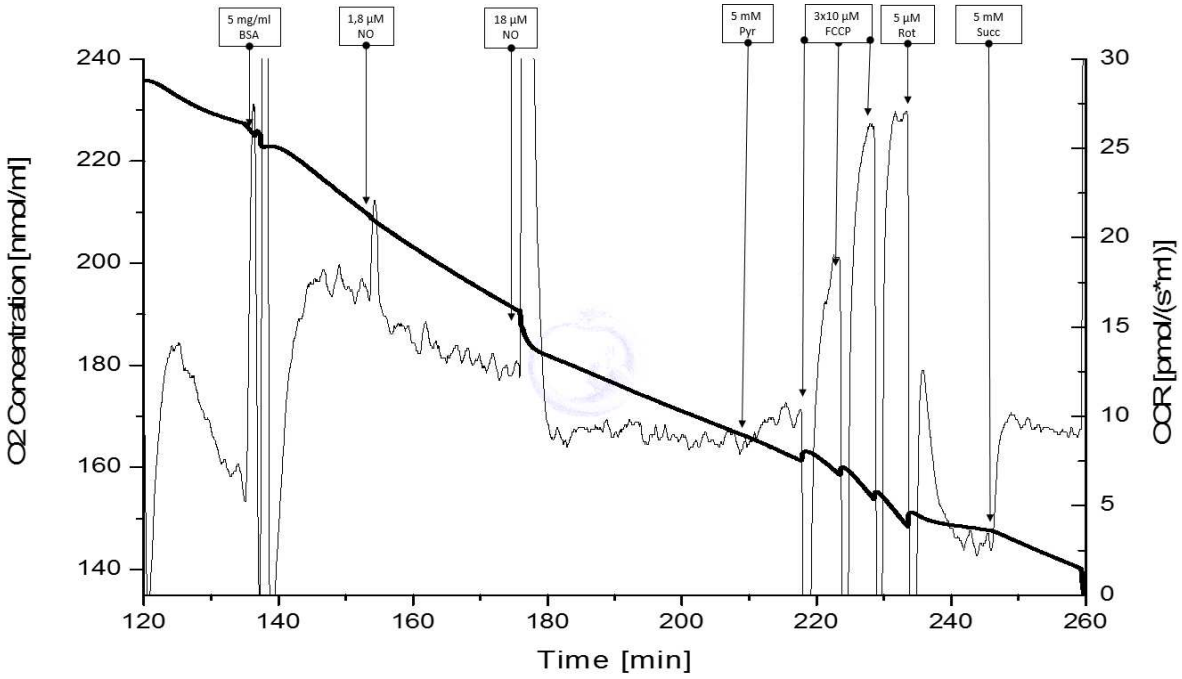

Figure 16. Effects of nitric oxide on the O_2 consumption rate under low O2 concentrations in 100 µm thick slices. The thick line is O_2 concentration (——) and the thin is line is the OCR (——). Successive titrations of 5 mg/ml fatty-acid free BSA, 1.8 µm •NO, 18 µm •NO, 5 mM pyruvate (Pyr), 30 µm FCCP, 5 µm rotenone (Rot), 5 mM pyruvate (Pyr) and 5 mM KCN.

4.2.2 Effects of glutamate on respiration

In accordance with the premise of the ANLSH, it has been suggested that glutamatergic neurotransmission is an inducer of aerobic glycolysis in certain brain areas[55] since glutamate is capable of inducing aerobic glycolysis in astrocytes. Using the capabilities of our system, we tested whether glutamate was able to induce an increase in oxidative metabolism or aerobic glycolysis in the tissue due to the proposed effect on astrocyte metabolism.

In a medium with 10 mM glucose, we titrated 50 mM glutamate (figure 18, A) and observed and increase in respiration of 14.2 ± 7,6% (n=2) in the FCR. These results show for the first time that glutamate induces an increase in OCR in acute hippocampal slices, using a system that maintains the cytoarchitecture and neuronal circuitry of the tissue.

With these results we can conclude that glutamate induces an increase in oxidative metabolism in the hippocampal tissue overall. This increase is probably due to increased energetic requirements of the cells in the tissue, as both neurons and astrocytes need large quantities of ATP for membrane potential regulation after a glutamate stimuli.

The observed increase in oxidative metabolism does not invalidate the occurrence of aerobic glycolysis in the tissue, but do show that the increase of oxidative metabolism is the major contributor to the shift on the OCR. Different results might have been obtained if we used a different brain area due to differences in cell types, for example, 72% of the cells of the cortex are nonneuronal cells while in the cerebellum, 80% of the cells are neurons[55]. We might expect to observe different results by performing this experiment in brain slices from these regions.

4.2.3 Respiration fuelled by lactate

The ANLSH proposes that after glutamatergic neurotransmission neurons change their primary substrate from glucose to lactate. To evaluate whether lactate can act as a primary substrate in hippocampal tissue in the basal state and after a glutamate stimulation, we recorded O_2 consumption in a medium with 20 mM lactate and compared the results with the ones obtained in a medium with 10 mM glucose.

We obtained the OCR for the basal respiration and then titrated 50 mM glutamate in both mediums to obtain the OCR for the glutamate-induced activation (figure 18). As can be observed in Figure 18, upon stimulation of neuronal activity by addition of glutamate to there is no significant difference ($p=0.420$) between OCR for slices supplemented with lactate or glucose. In the lactate medium, the OCR increase induced by glutamate was of 22.1 ± 10.0 % in FCR (n=3) and the increase induced in the medium of glucose was 14.2 ± 7.6 % in FCR (n=2). As for the ROUTINE state, there was not a significant difference ($p=0.854$) for the values obtained in the lactate medium and the glucose medium.

The ability of lactate to sustain brain cells even during evoked of action potentials in rat hippocampal slices has already documented[56], but we show here for the first time,

in a model which maintains the neuronal circuitry and cytoarchitectural organization of the tissue, that lactate is an oxidative substrate comparable to glucose in these conditions. Lactate was able to maintain the same rate of basal respiration, the ROUTINE state, as glucose and the increase in oxidative metabolism by glutamate was equally sustained by lactate and glucose.

These results suggest that lactate is a viable alternative to glucose as an oxidative substrate, this property of lactate may be important in cases of hypoglycemia where blood lactate may act has the fuel for brain activity, at least, for a short while. The lack of differences between the OCR's in the lactate fuelled and the glucose fuelled hippocampal slices, in both basal and stimulated conditions may indicate that neurons, astrocytes and other cells of the hippocampus have the required enzymatic machinery to use lactate has oxidative substrate, which may be useful data for the ANLSH and NALSH.

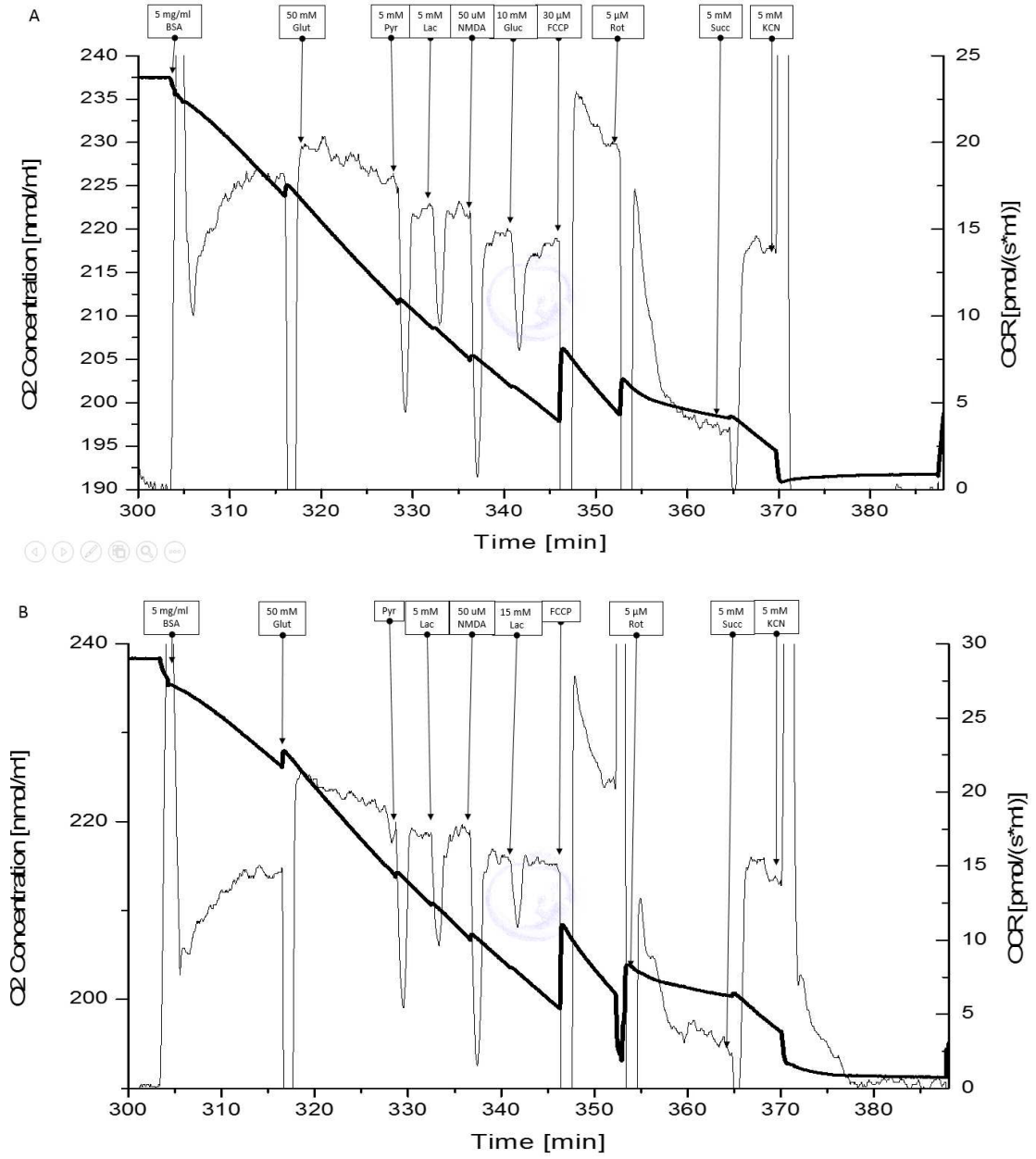

Figure 18. Comparison between basal respiration and glutamate-induced O_2 consumption in medium of lactate or glucose. The thick line represent O_2 concentration (——) and the thin line represents the OCR (——).The thicks line represent O_2 concentration (——) and the thin line represents the O_2 slope (——) We waited 15 minutes to obtain the OCR for basal respiration and then titrated 50 mM of glutamate to obtain the OCR for the activated neuronal tissue. To obtain a comparable OCR for the uncoupled state between the two experiments, we added either glucose or lactate in order to obtain an equal metabolite composition between the two media. (A) Medium supplemented with 20 mM lactate, with with successive titrations of 5 mg/ml fatty-acid free BSA, 50 mM glutamate (Glut), 5 mM pyruvate (Pyr), 5 mM lactate (Lac), 50 µM NMDA, 10 mM glucose (Gluc), 30 µm FCCP, 5 µm rotenone (Rot), 5 mM succinate (Succ) and 5 mM KCN. (B) Medium supplemented with 10 mM glucose, with successive titrations of 5 mg/ml fatty-acid free BSA, 50 mM glutamate (Glut), 5 mM pyruvate (Pyr), 5 mM lactate (Lac), 50 µM NMDA, 15 mM lac 30 µm FCCP, 5 µm rotenone (Rot), 5 mM succinate (Succ) and 5 mM KCN.

4.3 COMPARISON WITH OTHER WORKS

As the FCR's express respiratory control independent of mitochondrial content and cell size[32], we can compare the values obtained for the ROUTINE state, the RVI and RESIDUAL O_2 consumption with the values obtained from respirometry of intact cells present in the literature (Table I). By comparing our results with those obtained by others one can see that our value for the ROUTINE state is higher and has a higher standard deviation than those published by other groups.

Table I. Flux control ratios (FCRs) obtained for different intact cells from human, mouse and rat (mean ± SD)

Cell type	ROUTINE	RESIDUAL	REFERENCES
Transformed human embryonic kidney cells	0.31 ± 0.03	0.01 ± 0.01	([48])
Mouse parental hematopoietic cells	0.39 ± 0.02	0.03 ± 0.01	([33])
Human leukemia cells	0.40 ± 0.03	0.02 ± 0.03	([57])
Human umbilical vein endothelial cells	0.26 ± 0.02	0.05 ± 0.04	([35])
Human peritoneal mesothelial cells	0.40 ± 0.09	0.005 ± 0.01	([19])
Human foreskin fibroblasts	0.34 ± 0.03	0.07 ± 0.03	([36])
Rat Hippocampal Slices	0.58 ± 0.19	0.12 ± 0.16	

The high standard deviation may result from the heterogeneity of cell population present in acute brain slices.

As seen in Table I, the mean value obtained for the ROUTINE state in hippocampal slices are higher than those obtained by others in the cell cultures. It's

interesting to note that two relatively different approaches to hippocampal slice respirometry, the high O_2 concentrations using 200 µm slices and the lower O_2 concentrations with 100 µm thick slices, have close matching results for the values of the ROUTINE state. If this difference in the ROUTINE state between our experiments and the other works is due to the respiratory characteristic of the hippocampus, differences in general between cell culture preparations and acute tissue slice preparations or a still not fully optimized technique by our side is something that can only be answered with further experiments of acute brain slice respirometry.

5 CONCLUSIONS AND FUTURE WORK

In the work presented here we showed that glutamate-induced increase of neuronal activity increases O_2 consumption in rat hippocampal slices, suggesting an higher preeminence of oxidative metabolism than aerobic glycolysis as the mean to meet the increased energy demand of the tissue. We also showed that lactate can sustain the same rate of basal respiration as glucose and that the percentage increase of respiratory rate induced by glutamate is the same between the two subtracts, showing that the cells of the hippocampus have the required machinery to efficiently use lactate as a fuel for oxidative metabolism.

In terms of the unanswered questions of brain bioenergetics, the fact that apparently glutamatergic activation in the hippocampus induces mostly an increase in oxidative metabolism, rather than aerobic glycolysis is more easily justified in the light of the conventional theory of brain bioenergetics than either ANLSH or NALSH. However, a more detailed analysis of the relative increase of the glycolytic pathway would be required to fully answer this question. And the fact that lactate can be used as an efficient oxidative metabolism substrate, is not only favorable to the ANLSH and NALSH views, but may also be relevant in cases of hypoglycemia and impaired glucose metabolism.

The results shown here represent an improvement to previous work done using hippocampal slices in high-resolution respirometry experiments: the addition of the floater to support the tissue in the recording chamber allowed the slices to remain undamaged by the stirring bars, which was a problem in other works[58]. This is a critical aspect in maintaining healthy tissue, guaranteeing the maintenance of cytoarchitectural and circuitry integrity. The importance of maintaining this intercellular integrity derives from the fact that both ANLSH and NALSH are based on the fact that neurons and astrocytes most probably exchange/shuttle metabolic intermediates during increased activity states and that such an exchange is critical for neurons to maintain adequate energy production.

Respirometry of acute hippocampal slices using a different equipment, the Seahorse Extracellular Flux Analyser (Seahorse Bioscience) has been previously published, but the authors suspect that the acute brain slices suffered transient hypoxias for each cycle of medium reoxygenation, the same authors also performed intact cell respirometry using organotypic hippocampal slice cultures[59].

Regarding the future plans, the next step in optimizing this experimental technique would be to manufacture a floater to support the hippocampal slices made of a different material than doesn't adsorb oligomycin and other molecules with high partition coefficient. In comparison to polypropilene, polyvinylidene fluoride (PVDF) may be a good alternative as the material for the floater, as it appears to be less adsorbent than polypropylene, at least when comparing albumin adsorbance[60]. The nylon mesh has a low adsorbent tendency for albumin so it probably doesn't need to be replaced.

By solving the problem of oligomycin adsorbance to propylene we would be able measure the LEAK state. This would allow the comparison to be made between rat models of disease, testing for mitochondrial alterations in terms of O_2 consumption for oxidative phosphorylation versus O_2 consumed for proton pumping, giving information about the health of the mitochondria in the preparation.

As for metabolic profiling of the hippocampal slice, it would be interesting to be able to selectively block respiration in each cell type (neurons versus astrocytes). This might allow a better understanding of the primary substrate preferred by these cell types under basal conditions or in an activated state, helping to solve the doubts surrounding the conventional theory of brain energetics, ANLSH and the NALSH.

By using this approach in acute brain slices from other brain areas with different ratio of neuron-to-nonneuron cells, like the cortex and the cerebellum, it would be possible to understand if those areas have a higher or lower aerobic glycolysis after glutamate stimulation than what we observed in the hippocampus.

6 BIBLIOGRAPHY

1. Castro MA, Beltrán FA, Brauchi S, Concha II. A metabolic switch in brain: glucose and lactate metabolism modulation by ascorbic acid. Journal of Neurochemistry. 2009;110(2):423–440.

2. Attwell D, Laughlin SB. An energy budget for signaling in the grey matter of the brain. Journal of Cerebral Blood Flow and Metabolism. 2001;21(10):1133–1145.

3. Riedemann T, Patchev A V, Cho K, Almeida OFX. Corticosteroids: way upstream. Molecular Brain. 2010;3(2):1–20.

4. Abbott NJ, Patabendige A a K, Dolman DEM, Yusof SR, Begley DJ. Structure and function of the blood-brain barrier. Neurobiology of Disease. 2010;37(1):13–25.

5. Brown A, Ransom B. Astrocyte glycogen and brain energy metabolism. Glia. 2007;55(12):1263–1271.

6. Simpson IA, Carruthers A, Vannucci SJ. Supply and demand in cerebral energy metabolism: the role of nutrient transporters. Journal of Cerebral Blood Flow and Metabolism. 2007;27(11):1766–1791.

7. Chih C-P, Roberts EL. Energy substrates for neurons during neural activity: a critical review of the astrocyte-neuron lactate shuttle hypothesis. Journal of Cerebral Blood Flow and Metabolism. 2003;23(11):1263–1281.

8. Pellerin L, Magistretti PJ. Sweet sixteen for ANLS. Journal of Cerebral Blood Flow and Metabolism. 2012;32(7):1152–1166.

9. Almeida A, Cidad P, Bolaños JP. Nitric oxide accounts for an increased glycolytic rate in activated astrocytes through a glycogenolysis-independent mechanism. Brain Research. 2002;945(1):131–134.

10. Bolaños JP, Delgado-Esteban M, Herrero-Mendez A, Fernandez-Fernandez S, Almeida A. Regulation of glycolysis and pentose-phosphate pathway by nitric oxide: impact on neuronal survival. Biochimica et Biophysica Acta. 2008;1777(7-8):789–93.

11. Mangia S, Simpson IA, Vannucci SJ, Carruthers A. The in vivo neuron-to-astrocyte lactate shuttle in human brain: evidence from modeling of measured lactate levels during visual stimulation. Journal of Neurochemistry. 2009;109(Supplement 1):55–62.

12. Dienel GA, Hertz L. Glucose and lactate metabolism during brain activation. Journal of Neuroscience Research. 2001;66(5):824–838.

13. Dienel G. Brain lactate metabolism: the discoveries and the controversies. Journal of Cerebral Blood Flow & Metabolism. 2012;32(7):1107–38.

14. Almeida A, Almeida J, Bolaños JP, Moncada S. Different responses of astrocytes and neurons to nitric oxide: the role of glycolytically generated ATP in astrocyte protection. Proceedings of the National Academy of Sciences of the United States of America. 2001;98(26):15294–15299.

15. Castro M a, Angulo C, Brauchi S, Nualart F, Concha II. Ascorbic acid participates in a general mechanism for concerted glucose transport inhibition and lactate transport stimulation. Pflügers Archiv : European Journal of Physiology. 2008;457(2):519–28.

16. Nelson DL, Lehninger AL, Cox MM. Lehninger Principles of Biochemistry. 5th ed. W. H. Freeman; 2008 pp. 708–741.

17. Stryer L. Biochemistry. 4th ed. W.H. Freeman; 1995 pp. 529–558.

18. Opalka J, Gellerich F, Kling L, Muller-Beckmann B, Zierz S. Effect of the new matrix metalloproteinase inhibitor RO-28-2653 on mitochondrial function. Biochemical Pharmacology. 2002;63(4):725–732.

19. Stadlmann S, Renner K, Pollheimer J, Moser PL, Zeimet AG, Offner FA, Gnaiger E. Preserved coupling of oxidative phosphorylation but decreased mitochondrial respiratory capacity in IL-1β-treated human peritoneal mesothelial cells. Cell Biochemistry and Biophysics. 2006;44(3):179–186.

20. Clerc P, Polster BM. Investigation of mitochondrial dysfunction by sequential microplate-based respiration measurements from intact and permeabilized neurons. PloS one. 2012;7(4):1–8.

21. Gnaiger E. Bioenergetics at low oxygen: dependence of respiration and phosphorylation on oxygen and adenosine diphosphate supply. Respiration Physiology. 2001;128(3):277–297.

22. Rosenfeld E, Beauvoit B, Rigoulet M, Salmon J. Non-respiratory oxygen consumption pathways in anaerobically-grown Saccharomyces cerevisiae: evidence and partial characterization. Yeast. 2002;19(15):1299–1321.

23. Kabil O, Banerjee R. Redox biochemistry of hydrogen sulfide. The Journal of Biological Chemistry. 2010;285(29):21903–21907.

24. Mateo AO, De Artiñano MAA. Nitric oxide reactivity and mechanisms involved in its biological effects. Pharmacological Research. 2000;42(5):421–427.

25. Alderton WK, Cooper CE, Knowles RG. Nitric oxide synthases: structure, function and inhibition. The Biochemical Journal. 2001;357(Pt 3):593–615.

26. Garthwaite J. Concepts of neural nitric oxide-mediated transmission. The European Journal of Neuroscience. 2008;27(11):2783–802.

27. Guix FX, Uribesalgo I, Coma M, Muñoz FJ. The physiology and pathophysiology of nitric oxide in the brain. Progress in Neurobiology. 2005;76(2):126–152.

28. Martínez-Ruiz A, Cadenas S, Lamas S. Nitric oxide signaling: classical, less classical, and nonclassical mechanisms. Free Radical Biology & Medicine . 2011;51(1):17–29.

29. Sparling CE, Fedak MA. Metabolic rates of captive grey seals during voluntary diving. Journal of Experimental Biology. 2004;207(10):1615–1624.

30. Lighton JRB. Measuring Metabolic Rates : A Manual for Scientists.; 2008 pp. 7–62.

31. Oesper P. The History of the Warburg Apparatus. Journal of Chemical Education. 1964;41(6):294–296.

32. Pesta D, Gnaiger E. High-Resolution Respirometry: OXPHOS Protocols for Human Cells and Permeabilized Fibers from Small Biopsies of Human Muscle. In: Palmeira CM, J. Moreno A, editors. Mitochondrial Bioenergetics: Methods and Protocols. Humana Press; 2011. pp. 25–58.

33. Gnaiger E. Polarographic oxygen sensors, the oxygraph and high-resolution respirometry to assess mitochondrial function. In: Dykens JA, Will Y, editors. Drug-Induced Mitochondrial Dysfunction. ; 2008. pp. 327–348.

34. Friday E, Oliver III R, Turturro F, Welbourne T. Role of Glutamate Dehydrogenase in Cancer Growth and Homeostasis. In: Canuto RA, editor. Dehydrogenases.2012.

35. Hütter E, Unterluggauer H, Garedew A, Jansen-Dürr P, Gnaiger E. High-resolution respirometry--a modern tool in aging research. Experimental gerontology. 2006;41(1):103–9.

36. Hutter E, Renner K, Pfister G, Stöckl P, Jansen-Dürr P, Gnaiger E. Senescence-associated changes in respiration and oxidative phosphorylation in primary human fibroblasts. The Biochemical Journal. 2004 June 15;380(Pt 3):919–28.

37. Vesce S, Jekabsons MB, Johnson-Cadwell LI, Nicholls DG. Acute glutathione depletion restricts mitochondrial ATP export in cerebellar granule neurons. The Journal of Biological Chemistry. 2005;280(46):38720–38728.

38. Amaral D, Lavenex P. Hippocampal Neuroanatomy. In: Andersen P, editor. The Hippocampus Book. ; 2007. pp. 37–104.

39. Gloveli T, Dugladze T, Rotstein HG, Traub RD, Monyer H, Heinemann U, Whittington M a, Kopell NJ. Orthogonal arrangement of rhythm-generating microcircuits in the hippocampus. Proceedings of the National Academy of Sciences of the United States of America. 2005;102(37):13295–13300.

40. De Vivo L, Melone M, Rothstein JD, Conti F. GLT-1 Promoter Activity in Astrocytes and Neurons of Mouse Hippocampus and Somatic Sensory Cortex. Frontiers in Neuroanatomy. 2010;3(31):1–9.

41. Nagy JI. Evidence for connexin36 localization at hippocampal mossy fiber terminals suggesting mixed chemical/electrical transmission by granule cells. Brain research. 2012;1487:107–22.

42. Mulkey D, Henderson R, Olson JE, Putnam RW, Dean JB. Oxygen measurements in brain stem slices exposed to normobaric hyperoxia and hyperbaric oxygen. Journal of Applied Physiology. 2001;90(5):1887–1899.

43. Kadar EP, Su Y, Zhang Y, Tweed J, Wujcik CE. Evaluation of the relationship between a pharmaceutical compound's distribution coefficient, log D and adsorption loss to polypropylene in urine and CSF. Bioanalysis. 2010;2(4):755–67.

44. Anon. ADC/Log P, version 10, Advanced Chemistry Development, Inc., Toronto, ON, Canada, www.acdlabs.com, 2013.

45. Ledo A, Barbosa R, Cadenas E, Laranjinha J. Dynamic and interacting profiles of *NO and O2 in rat hippocampal slices. Free Radical Biology & Medicine. 2010;48(8):1044–1050.

46. Takehara Y, Kanno T, Yoshioka T, Inoue M, Utsumi K. Oxygen-dependent regulation of mitochondrial energy metabolism by nitric oxide. Archives of Biochemistry and Biophysics. 1995;323(1):27–32.

47. Brown GC, Cooper CE. Nanomolar concentrations of nitric oxide reversibly inhibit synaptosomal respiration by competing with oxygen at cytochrome oxidase. FEBS letters. 1994;356(2-3):295–298.

48. Aguirre E, Rodríguez-Juárez F, Bellelli A, Gnaiger E, Cadenas S. Kinetic model of the inhibition of respiration by endogenous nitric oxide in intact cells. Biochimica et Biophysica Acta. 2010;1797(5):557–65.

49. Kharitonov VG, Sundquist a R, Sharma VS. Kinetics of nitric oxide autoxidation in aqueous solution. The Journal of Biological Chemistry. 1994;269(8):5881–3.

50. Ignarro LJ, Fukuto JM, Griscavage JM, Rogers NE, Byrns RE. Oxidation of nitric oxide in aqueous solution to nitrite but not nitrate: comparison with enzymatically formed nitric oxide from L-arginine. Proceedings of the National Academy of Sciences of the United States of America. 1993;90(17):8103–8107.

51. Schwartzkroin PA. Epilepsy: Models, Mechanisms and Concepts. Cambridge University Press; 2007 p. 185.

52. Brown GC. Nitric oxide and mitochondrial respiration. Biochimica et Biophysica Acta. 1999;1411(2-3):351–369.

53. Riobó N, Clementi E, Melani M, Boveris A, Cadenas E, Moncada, S. Nitric oxide inhibits mitochondrial NADH: ubiquinone reductase activity through peroxynitrite formation. Biochemistry Journal. 2001;145(Pt 1):139–145.

54. Cassina A, Radi R. Differential inhibitory action of nitric oxide and peroxynitrite on mitochondrial electron transport. Archives of Biochemistry and Biophysics. 1996;328(2):309–316.

55. Vaishnavi SN, Vlassenko AG, Rundle MM, Snyder AZ, Mintun M a, Raichle ME. Regional aerobic glycolysis in the human brain. Proceedings of the National Academy of Sciences of the United States of America. 2010;107(41):17757–17762.

56. Izumi Y, Benz AM, Katsuki H, Zorumski CF. Endogenous Monocarboxylates Sustain Hippocampal Synaptic Function and Morphological Integrity during Energy Deprivation. The Journal of Neuroscience. 1997;17(24):9448–9457.

57. Renner K, Amberger A, Konwalinka G, Kofler R, Gnaiger E. Changes of mitochondrial respiration, mitochondrial content and cell size after induction of apoptosis in leukemia cells. Biochimica et Biophysica Acta. 2003;1642(1-2):115–123.

58. Kudin AF, Vielhaber S, Beck H, Elger CE. Quantitative investigation of mitochondrial function in single rat hippocampal slices: a novel application of high-resolution respirometry and laser-excited fluorescence. Brain Research Protocols. 1999;4(3):329–334.

59. Schuh R a, Clerc P, Hwang H, Mehrabian Z, Bittman K, Chen H, Polster BM. Adaptation of microplate-based respirometry for hippocampal slices and analysis of respiratory capacity. Journal of Neuroscience Research. 2011;89(12):1979–88.

60. Johansson J, Yasuda H, Bajpai R. Fouling and Protein Adsorption. Applied Biochemistry and Biotechnology. 1998;70(2):747–763.